AIChE Letter: Soft Matter: Synthesis, Processing, and Products

Cooperative Catalytic Activity of Cyclodextrin and Ag Nanoparticles Immobilized on Spherical Polyelectrolyte Brushes

Jianjia Liu, Jie Wang, Zhongming Zhu, Li Li, and Xuhong Guo
State Key Laboratory of Chemical Engineering, School of Chemical Engineering, East China University of Science and Technology, Shanghai 200237, China

Stephen F. Lincoln
School of Chemistry and Physics, University of Adelaide, Adelaide, SA 5005, Australia

Robert K. Prud'homme
Dept. of Chemical Engineering, Princeton University, Princeton, NJ 08544

DOI 10.1002/aic.14465
Published online April 19, 2014 in Wiley Online Library (wileyonlinelibrary.com)

Significance

Spherical polyelectrolyte brushes (SPB) loaded with silver nanoparticles (Ag-NP) were synthesized, and they were characterized in aqueous solution using TEM, ICP-AES and UV-vis spectroscopy. While the size distribution of the Ag-NP synthesized at a given temperature is quite uniform this distribution varies with change in synthesis temperature. The Ag-NP have a strong catalytic effect on the reduction of 4-nitrophenol to 4-aminophenol by NaBH4. The addition of α-cyclodextrin (α-CD) further accelerates this 4-nitrophenol reduction and modifies the associated activation parameters. This is attributed to α-CD complexing 4-nitrophenol in the vicinity of the Ag-NP surface and thereby aiding the catalysis. *AIChE J*, 60: 1977–1982, 2014
Keywords: spherical polyelectrolyte brush, α-cyclodextrin, silver nanoparticle, catalysis

Introduction

Metal nanoparticles have been the subject of intense interest in recent years partially as a consequence of their efficient catalytic properties[1–3] which arise substantially from their high surface-to-volume ratio.[4,5] However, the catalytic properties of free metal nanoparticles is diminished on aggregation and as a consequence several systems including polymers,[6] dendrimers,[7] microgels,[8] and colloids[9] have been studied as carrier systems which substantially diminish this aggregation and thereby retain metal nanoparticle catalytic activity. In the light of this knowledge, we are interested in exploring to what extent such catalytic activity may be increased.

Recently, spherical polyelectrolyte brushes (SPBs) have been reported as novel carriers which generate well-defined metal nanoparticles with a narrow-size distribution *in situ* and also immobilizes them.[10–13] Such metal nanoparticles catalyze the reduction of 4-nitrophenol (4-NP) to 4-aminophenol (4-AP) which is an important industrial reaction.[14,15] In this study, we find that α-cyclodextrin (α-CD), a six-membered cyclic oligomer of α-1,4-linked-D-glycopyranose[16,17] which forms host-guest complexes with a wide range of hydrophobic guest species through noncovalent interactions[18–21] increases the rate of the catalytic reduction of 4-NP to 4-AP by silver nanoparticles (Ag-NPs) immobilized on SPBs. Studies of Ag and Au nanoparticles suggest that the less polar primary α-CD faces bind to the nanoparticle apolar surfaces.[22,23] On this basis, the wider and more polar α-CD secondary faces are exposed to bind suitable guest species such as 4-NP in the α-CD annulus and in close proximity to the catalytic surface and thereby enhance the probability of reduction by $NaBH_4$ in the mechanism proposed for the increased catalysis rate shown in Figure 1. On a statistical basis, up to three α-CDs are expected to bind to the Ag-NP surface under the conditions of the study.

Experimental

Synthesis of the SPBs was carried out in three steps as described in the literature.[24,25] First, the polystyrene core latexes were synthesized using a conventional emulsion

Correspondence concerning this article should be addressed to J. Wang at jiewang2010@ecust.edu.cn or X.H. Guo at guoxuhong@ecust.edu.cn.

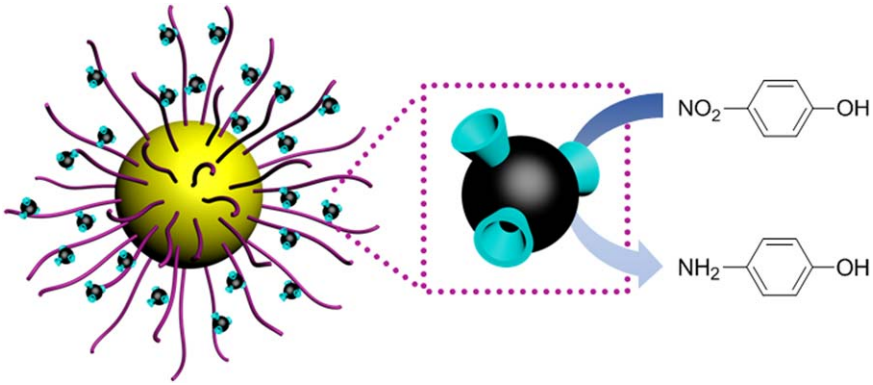

Figure 1. Schematic illustration of the proposed mechanism for cooperative catalytic activity of α-CD and Ag-NP immobilized on SPBs in converting 4-NP to 4-AP in the presence of $NaBH_4$ based on a maximum external diameter of 1.5 nm for α-CD and a diameter of 3 nm for Ag-NP and the relative concentrations of these species pertaining to this study.

[Color figure can be viewed in the online issue, which is available at wileyonlinelibrary.com.]

polymerization of styrene. Second, a thin shell of photoinitiator, 2[*p*-(2-hydroxy-2-methylpropiophenone)]ethyleneglycolmethacrylate (HMEM) was added to the polystyrene latex core. Third, the HMEM-modified polystyrene latex cores and acrylic acid were mixed in a UV-reactor. Finally, photoemulsion polymerization was accomplished through UV radiation at room temperature with vigorous stirring to give the SPBs.

In a typical Ag-NP preparation, 0.012 g of NaOH was added to 50 cm^3 of a 1.1 wt % aqueous solution of SPBs to neutralize the carboxylic acid groups of the polyacrylic acid strands. After stirring for 10 h, the mixture was washed with 3.0 dm^3 of aqueous 0.001 mol dm^{-3} $AgNO_3$ solution to replace Na^+ by Ag^+ in an ultrafiltration cell. This was followed by washing with large amounts of distilled water to remove excess $AgNO_3$. Silver nanoparticles were produced through the slow addition of 0.2 g of $NaBH_4$ dissolved in 5.0 cm^3 of water to 50 cm^3 of an aqueous SPB (1.1 wt %) solution stirred at 400 r min^{-1} under nitrogen and thermostated at either 273.15, 303.15, or 333.15 K. The formation of the Ag-NP was followed by the appearance of a plasmon resonance absorption as shown in Figure 2.[14,26]

In the kinetic experiments, 3.0 cm^3 of an aqueous solution of 4-NP (1.0×10^{-4} mol dm^3) and $NaBH_4$ (2.0×10^{-2} mol dm^3) in a thermostated quartz cuvette was purged with N_2 for 5 min to remove dissolved oxygen after which the solution pH was 10.2. The solution was then made 1.01×10^{-6} mol dm^{-3} in Ag by the addition of 6 mm^3 of a Ag-NP-loaded SPB stock solution 5.03×10^{-4} mol dm^{-3} in Ag. (This solution was the comparison solution for the 4-NP reduction kinetic studies.) Under the same conditions, 5.0, 6.0, 7.0, and 8.0 mm^3 of a 1.35×10^{-3} mol dm^{-3} α-CD stock solution were added to four other solutions to make them (2.25, 2.70, 3.15, and 3.60) $\times 10^{-6}$ mol dm^{-3} in [α-CD]. The concentration of Ag in these five solutions was determined to be 0.11 mg dm^{-3} from ICP-AES (Varian 710 ES) measurements. Immediately, after the addition of the Ag-NPs, the reduction of 4-NP was followed by the decrease in absorbance at 400 nm with time. It should be noted that this absorbance arises from 4-nitrophenolate in protonic equilibrium with 4-nitrophenol ($pK_a = 7.15$)[27] and that at the concentration of Ag-NPs employed their plasmon resonance absorbance is insignificant by comparison.

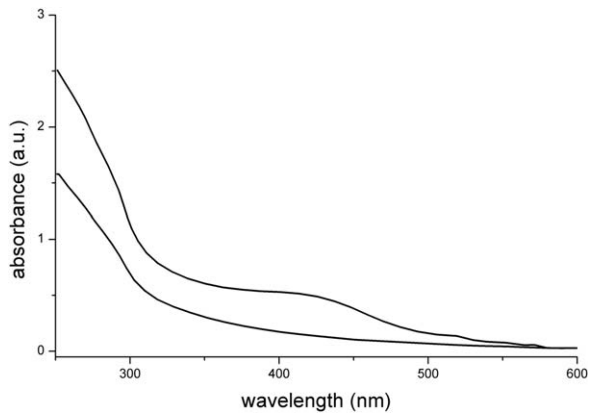

Figure 2. UV-vis spectrum of a $AgNO_3$–SPB solution before (lower curve) and after reduction (upper curve).

Results and Discussion

Silver nanoparticles were synthesized at 273.15, 303.15, and 333.15 K by addition of $NaBH_4$ to SPBs loaded with Ag^+ (Figure 3). The morphology of the Ag-NPs resulting from the Ag^+ reduction was determined by TEM which showed their immobilization as indicated by the dark points dispersed within the Ag-NP-loaded SPBs, or Ag-NP-SPBs, (Figure 4). The histograms calculated from the TEM images, show a narrow-size distribution with the dominant Ag-NP diameter being 2.5 nm at 273.15 K, 2.8 nm at 303.15 K, and 3.1 nm at 333.15 K. When the reaction temperature was decreased from 333.15 to 273.15 K, the generation of Ag-NPs slowed as shown from the decreased rate of growth of the plasmon resonance absorption. The Ag-NP size decreased and the size distribution became narrower as temperature decreased (Figure 4). Thus, both the size and the size distribution of Ag-NPs may be controlled through the temperature at which the reduction of Ag^+ ions occurs.

To test the catalytic properties of the Ag-NPs (synthesized at 303.15 K) and the effect of α-CD on catalysis, the kinetics of the reduction reaction were monitored by UV-vis spectroscopy in the absence of α-CD and at four [α-CD] over the temperature range 283.15–303.15 K. After addition of the Ag-NP-SPBs, the peak at 400 nm originated from 4-nitrophenolate decreased with time and a new peak at 300

nm arising from the 4-aminophenol product[28] increased proportionately (Figure 5a). Four isosbestic points at 222, 247, 281, and 313 nm indicate the generation of a dominant product, 4-AP, in the reaction. Two typical rate plots appear in Figure 5b where k_1 for the 4-NP reduction in the absence of α-CD was 0.061 $dm^3\ s^{-1}\ m^{-2}$ which compares with 0.11 $dm^3\ s^{-1}\ m^{-2}$ in the presence of 2.70×10^{-6} mol dm^{-3} α-CD at 293.15 K. Because the initial [$NaBH_4$] was in 200-fold excess over the initial [4-NP], the reduction was pseudofirst-order according to Eq. 1 where k_{app} is the apparent rate constant, c_t is [4-NP] at time t and k_1 is normalized to the Ag-NP of diameter 2.8 nm and a surface area $S = 0.022\ m^2\ dm^{-3}$.

$$-dc_t/dt = k_{app}\, c_t = k_1 S c_t \tag{1}$$

The rate constant k_1 increases with temperature both in the absence and presence of α-CD, but for a particular temperature the profile of the increase in k_1 over the range 10^6 [α-CD] = 0, 2.25, 2.70, 3.15, and 3.60 mol dm^3 range varies as seen in Figure 6a. Thus, at 283.15 K, the dependence of k_1 on [α-CD] appears to level out as [α-CD] increases, whereas at 293.15 K the dependence of k_1 on [α-CD] approaches linearity, and at 298.15 K and 303.15 K the dependence of k_1 on [α-CD] becomes linear and the increase in k_1 with increase in [α-CD] diminishes with increase in temperature. This is consistent with the temperature dependence of k_1 on [α-CD] being subject to temperature-dependent variables additional to the temperature dependence expected from the Arrhenius equation (Eq. 2) the reduction alone. Such variables are likely to include the motion of the polyacrylate strands which may influence the approach of both 4-NP and $NaBH_4$ to the Ag-NP surface, the binding of α-CD to the Ag-NP surface (which in turn varies the relative contributions to k_1 of the catalysis on the Ag-NP surface and through α-CD bound to the Ag-NP surface), and the binding of 4-NP in the α-CD annulus. In aqueous solution, the binding of 4-nitrophenol and 4-nitrophenolate by α-CD is characterized by binding constants of 220 and 1800 $dm^3\ mol^{-1}$ at 298.2 K, respectively,[18] but it is possible that the strength of binding may change in the environment of the Ag-NP.

$$k_1 = Ae^{-Ea/RT} \tag{2}$$

Plots of $\ln k_1$ against $1/T$ for each [α-CD] shown in Figure 6b yield the activation energies, E_a, and preexponential factors, A, through the Arrhenius equation (Eq. 2) as shown in Table 1. There is a substantial decrease from the E_a observed in the absence of α-CD to the four E_a values observed in the presence of α-CD which are identical within experimental error. Correspondingly, the value of A decreases by three orders of magnitude on addition of α-CD to the reaction solutions which is consistent with a significant degree of ordering occurring in the activated state in the presence of α-CD which is consistent with 4-NP bound in α-CD sited on the Ag-NP surface. This major change in the activation energetics of the 4-NP reduction caused by α-CD may reflect a change of hydration of 4-NP bound in the α-CD annulus combined with a change in the mechanism of reaction of 4-NP and hydride ions on the Ag-NP surface.

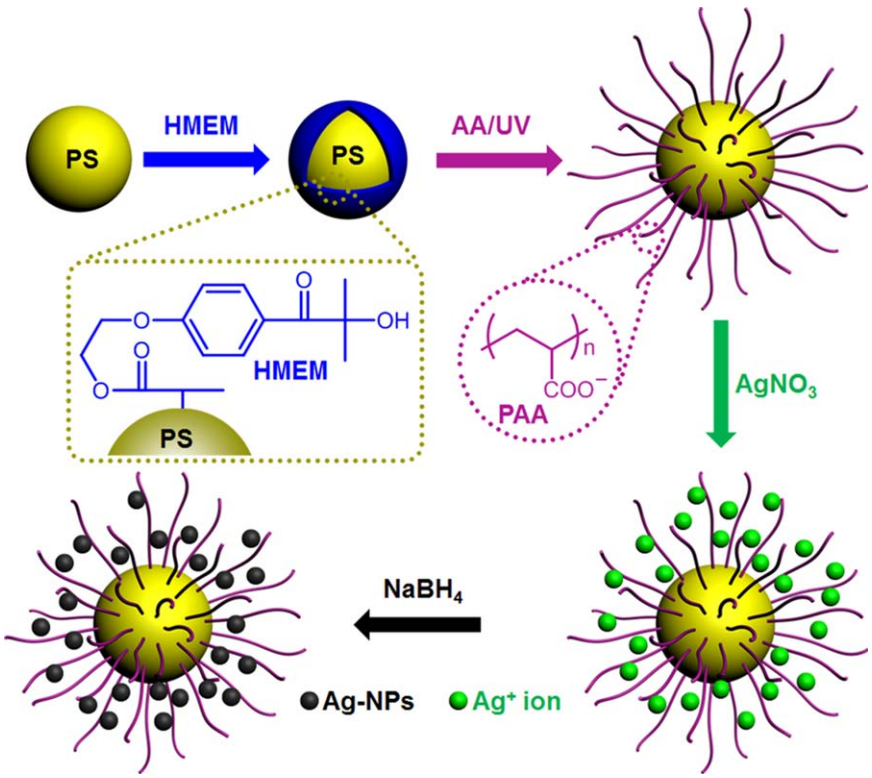

Figure 3. Schematic representation of the synthesis of the SPBs and the loading of Ag-NPs inside the SPBs.

[Color figure can be viewed in the online issue, which is available at wileyonlinelibrary.com.]

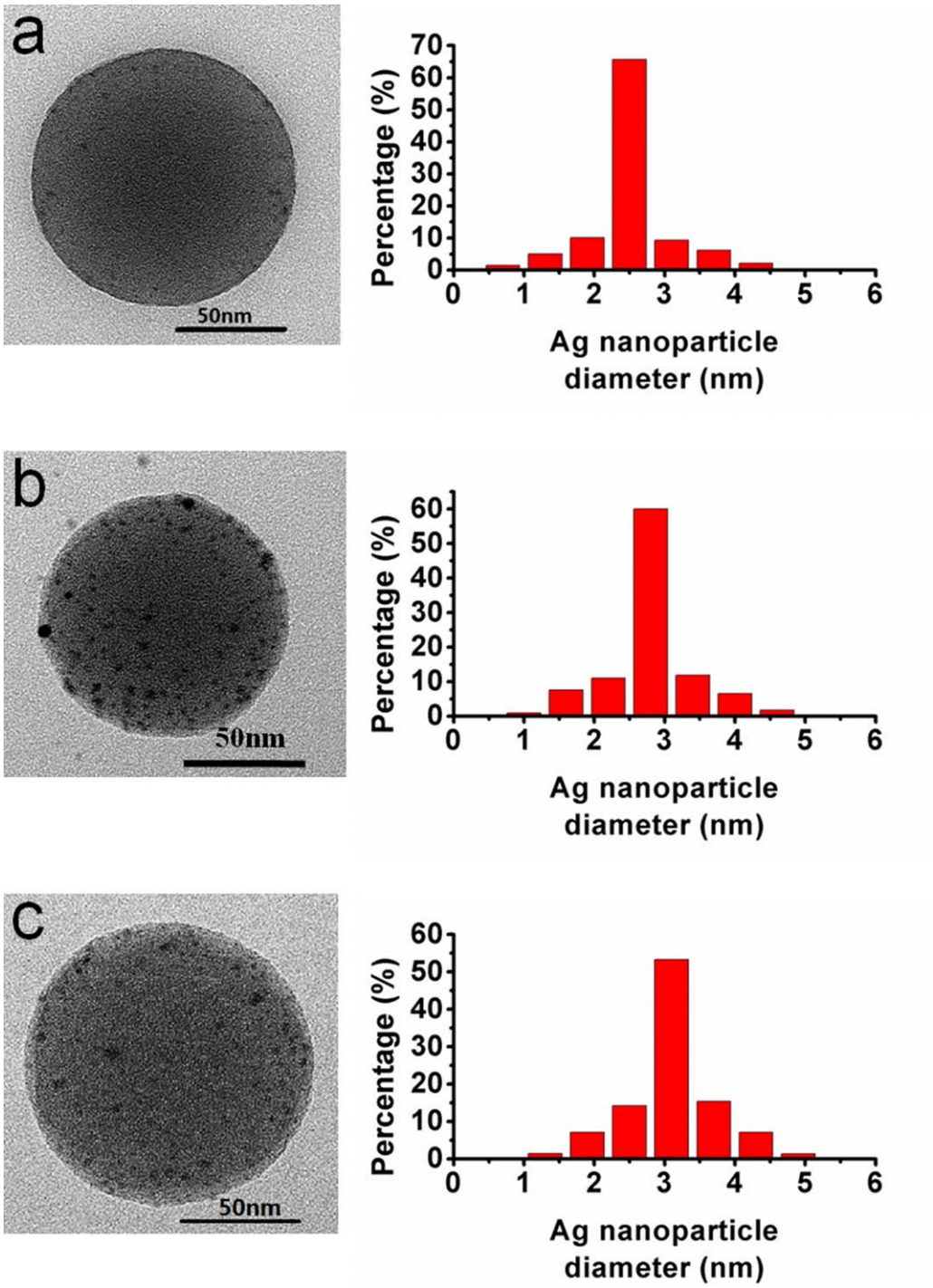

Figure 4. TEM images of Ag-NP-SPBs, showing Ag-NPs as small dark spheres within the SPBs at (a) 273.15, (b) 303.15, and (c) 333.15 K and the corresponding histograms Ag-NP of size distribution.

[Color figure can be viewed in the online issue, which is available at wileyonlinelibrary.com.]

It is of interest to speculate about the role that the larger β- and γ-cyclodextrins, β-CD and γ-CD, might play in similar studies. The binding constants for 4-NP and its phenolate by β-CD are 350 and 570 $dm^3\ mol^{-1}$, respectively, at 298.2 K and are larger and smaller, respectively, than the analogous binding constants for α-CD under the same conditions.[18] As a similar number of α-CD and β-CD are likely to be accommodated on the Ag-NP surface, it is anticipated that influence of both CDs on the 4-NP process would have some similarity. However, as there are substantial differences in the corresponding ΔH and ΔS for binding between the two systems,[18] the temperature dependences of the catalyzed

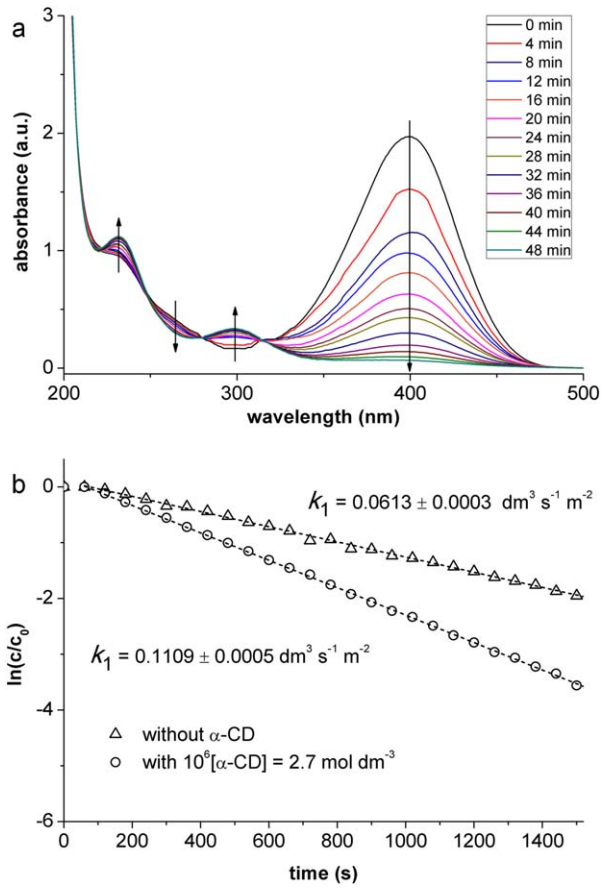

Figure 5. (a) Time dependence of the UV-vis spectra arising from the reduction of [4-NP] = 1.0 × 10^{-4} mol dm^{-3} by [$NaBH_4$] = 2.0 × 10^{-2} mol dm^{-3} in the presence of Ag-NP-SPBs. [Ag] = 0.11 mg dm^{-3} and [α-CD] = 2.70 × 10^{-6} mol dm^{-3} at 293.15 K.

The arrows indicate the direction of absorbance changes with increasing time. (b) Comparison of $\ln(c_t/c_0)$ vs. time for the reduction of 4-NP in the absence of α-CD and in the presence of [α-CD] = 2.70 × 10^{-6} mol dm^{-3} but otherwise under the same conditions as for (a). The errors shown for k_1 are the fitting errors. The overall experimental error in k_1 is estimated to be ±3%. [Color figure can be viewed in the online issue, which is available at wileyonlinelibrary.com.]

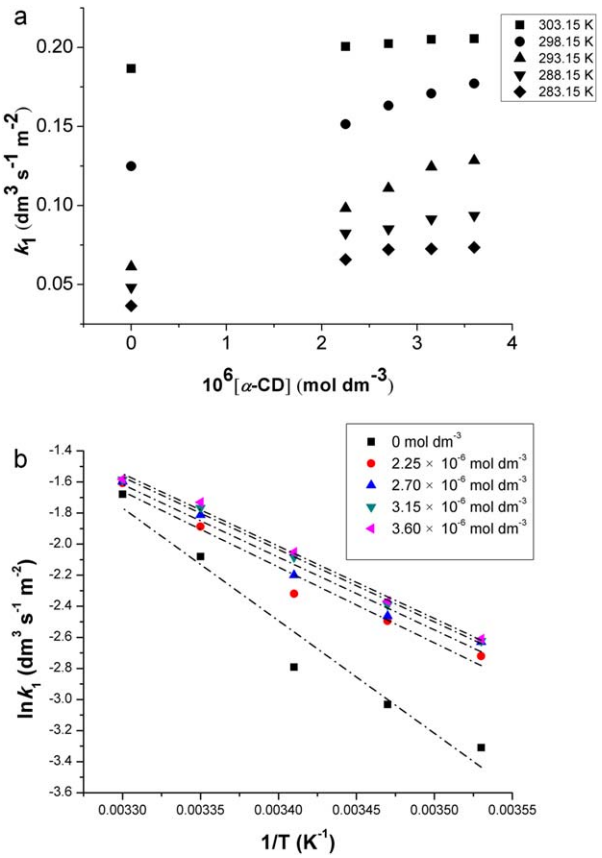

Figure 6. (a) Effect of the variation of 10^6[α-CD] in the range 0, 2.25, 2.70, and 3.15 to 3.60 mol dm^{-3} on k_1 at different temperatures.

For each reaction [4-NP] = 1.0 × 10^{-4} mol dm^{-3}, [$NaBH_4$] = 2.0 × 10^{-2} mol dm^{-3}, and [Ag] = 0.11 mg dm^{-3}. (b) Plot of $\ln k_1$ vs. $1/T$ for the reduction of 4-NP at different [α-CD] with the best fits of the Arrhenius equation to the data represented by broken lines. [Color figure can be viewed in the online issue, which is available at wileyonlinelibrary.com.]

reduction of 4-NP might differ. The substantially larger size of γ-CD, as illustrated by its annular volume of 427 $Å^3$ compared with 174 and 262 $Å^3$ for α-CD and β-CD,[21] is likely to cause a degree of crowding on the Ag-NP surface. This, in combination with the larger annular volume of γ-CD, is likely to change the extent of 4-NP binding and thereby change the catalysis characteristics.

Conclusions

The Ag-NPs immobilized in the SPBs catalyze the reduction by $NaBH_4$ of 4-NP to 4-AP, and the addition of α-CD accelerates the reaction rate. This acceleration is attributable to the binding of α-CD through its primary face to the Ag surface and the subsequent binding of 4-NP for a period

Table 1. Variation of Activation Energy, *E*a, and Preexponential Factor, *A*, with [α-CD]

[α-CD] mol dm^{-3}	0	2.25 × 10^{-6}	2.70 × 10^{-6}	3.15 × 10^{-6}	3.60 × 10^{-6}
k_1 (298.15 K)[a] min^{-1}	0.1249 ± 0.0071	0.1515 ± 0.0053	0.1632 ± 0.0039	0.1709 ± 0.0008	0.1772 ± 0.0015
*E*a[a] KJ	60.27 ± 3.42	40.55 ± 1.43	38.91 ± 0.92	38.78 ± 0.19	38.73 ± 0.32
A[a] s^{-1}	(4.1726 ± 0.2370) × 10^9	(1.8565 ± 0.0655) × 10^6	(1.0128 ± 0.0240) × 10^6	(1.0083 ± 0.0048) × 10^6	(1.0080 ± 0.0083) × 10^6

[a]Fitting errors. The minimum experimental error in determining k_1 at given temperature is estimated to be ±5%.

substantially greater than a collision time such that the probability of reduction by $NaBH_4$ is significantly increased. The temperature dependence of the rate of 4-NP reduction is complex and is likely to include changes in the motion of the polyacrylate strands of the SPB which may influence interactions between 4-NP and $NaBH_4$ on the Ag-NP surface, the binding of α-CD to the Ag-NP surface, and binding of 4-NP in the α-CD annulus, all of which have their separate temperature dependences. Although this is clearly a complex system, our preliminary study provides new insight into catalytic activity on metal nanoparticle surfaces and its enhancement. This provides a basis for future studies of the effect of different CDs and metals on the catalytic effect of metal nanoparticles immobilized in SPBs.

Acknowledgments

The authors gratefully acknowledge the NSFC Grants 51273063 and 20774030, the Fundamental Research Funds for the Central Universities, the higher school specialized research fund for the doctoral program (20110074110003), the China Scholarship Council, and the Australian Research Council Grant DP110103177 for funding this work.

Literature Cited

1. Ho CH, Tobis J, Sprich C, Thomann R, Tiller JC. Nanoseparated polymeric networks with multiple antimicrobial properties. *Adv Mater*. 2004;16:957–961.
2. Burda C, Chen X, Narayanan R, El-Sayed MA. Chemistry and properties of nanocrystals of different shapes. *Chem Rev*. 2005;105:1025–1102.
3. Sardar R, Funston AM, Mulvaney P, Murray RW. Gold nanoparticles: past, present, and future. *Langmuir*. 2009; 25:13840–13851.
4. Campbell CT, Parker SC, Starr DE. The effect of size-dependent nanoparticle energetics on catalyst sintering. *Science*. 2002;298:811–814.
5. Mayer ABR, Mark JE, Hausner SH. Colloidal platinum-polyacid nanocatalyst systems. *Angew Makromol Chem*. 1998;259:45–53.
6. Vincent T, Guibal E. Chitosan-supported palladium catalyst 3. Influence of experimental parameters on nitrophenol degradation. *Langmuir*. 2003;19:8475–8483.
7. Scott RWJ, Wilson OM, Crooks RM. Synthesis, characterization, and applications of dendrimer-encapsulated nanoparticles. *J Phys Chem B*. 2005;109:692–704, and references therein.
8. Zhang J, Xu S, Kumacheva E. Polymer microgels: reactors for semiconductor, metal, and magnetic nanoparticles. *J Am Chem Soc*. 2004;126:7908–7914.
9. Liang Z, Susha A, Caruso F. Gold nanoparticle-based core-shell and hollow spheres and ordered assemblies thereof. *Chem Mater*. 2003;15:3176–3183.
10. Sharma G, Ballauff M. Cationic spherical polyelectrolyte brushes as nanoreactors for the generation of gold particles. *Macromol Rapid Commun*. 2004;25:547–552.
11. Zhu Z, Guo XH, Wu S, Zhang R, Wang J, Li L. Preparation of nickel nanoparticles in spherical polyelectrolyte brush nanoreactor and their catalytic activity. *Ind Eng Chem Res*. 2011;50:13848–13853.
12. Wu S, Kaiser J, Guo XH, Li L, Lu Y, Ballauff M. Recoverable platinum nanocatalysts immobilized on magnetic spherical polyelectrolyte brushes. *Ind Eng Chem Res* 2011;51:5608–5614.
13. Li GS, Xu J, Zhao SF, Zhu YQ, Li L, Guo XH. Spherical polyelectrolyte brushes on colloidal poly(butadiene) particles. *Z Phys Chem*. 2012;226:613–623.
14. Lu Y, Mei Y, Ballauff M, Drechsler M. Thermosensitive core-shell particles as carrier systems for metallic nanoparticles. *J Phys Chem B*. 2006;110:3930–3937.
15. Rode C, Vaidya M, Jaganathan R, Chaudhari R. Hydrogenation of nitrobenzene to *p*-aminophenol in a four-phase reactor: reaction kinetics and mass-transfer effects. *Chem Eng Sci*. 2001;56:1299–1304.
16. Szejtli J. Introduction and general overview of cyclodextrin chemistry. *Chem Rev*. 1998;98:1743–1754.
17. Easton CJ, Lincoln SF. *Modified Cyclodextrins: Scaffolds and Templates for Supramolecular Chemistry*. London: Imperial College Press, 1999.
18. Bertrand BL, Faulkner JR, Han SM, Armstrong DW. Substituent effects on the binding of phenols to cyclodextrins in aqueous solution. *J Phys Chem*. 1989;93: 6863–6867.
19. Rekharsky MV, Inoue Y. Complexation thermodynamics of cyclodextrins. *Chem Rev* 1998;98:1875–1917.
20. Wenz G, Han BH, Muller A. Cyclodextrin rotaxanes and polyrotaxanes. *Chem Rev* 2006;106:782–817.
21. Lincoln SF, Pham, D-T. Cyclodextrins: From nature to nanotechnology. In: Gale PA, Steed JW, editors. *Supramolecular Chemistry: From Molecules to Nanomaterials*. Chichester: Wiley, 2012:955–982.
22. Ng CHB, Yang J, Fan WY. Synthesis and self-assembly of one-dimensional sub-10 nm Ag nanoparticles with cyclodextrin. *J Phys Chem C*. 2008;112:4141–4145.
23. Huang T, Meng F, Qi L. Facile synthesis and one-dimensional assembly of cyclodextrin-capped gold nanoparticles and their applications in catalysis and surface-enhanced Raman scattering. *J Phys Chem C*. 2009;113: 13636–13642.
24. Guo X, Weiss, A, Ballauff M. Synthesis of spherical polyelectrolyte brushes by photoemulsion polymerization. *Macromolecules*. 1999; 32:6043–6046.
25. Wang X, Wu S, Li L, Zhang R, Zhu Y, Ballauff M, Lu Y, Guo XH. Synthesis of spherical polyelectrolyte brushes by photoemulsion polymerization with different photoinitiators. *Ind Eng Chem Res*. 2011;50:3564–3569.
26. Amendola V, Bakr OM, Stellacei, F. A study of the surface plasmon resonance of silver nanoparticles by the discrete dipole approximation method: effect of shape, size, structure, and assembly. *Plasmonics*. 2010;5:88–97.
27. Albert A, Serjeant EP. *Ionization Constants of Organic Bases in Aqueous Solution*. London: Butterworth, 1965.
28. Wunder S, Polzer F, Lu Y, Mei Y, Ballauff M. Kinetic analysis of catalytic reduction of 4-nitrophenol by metallic nanoparticles immobilized in spherical polyelectrolyte brushes. *J Phys Chem C*. 2010;114:8814–8820.

Received Sept. 27, 2013, and revision received Mar. 6, 2014,